Title: Comparative thermal performance of *Orbicella franksi* at its latitudinal range limits

Running title: Comparative thermal performance of *O. franksi*

Nyssa J. Silbiger*[1], Gretchen Goodbody-Gringley[2], John F. Bruno[3], Hollie M. Putnam[4]

[1]Department of Biology, California State University, 18111 Nordhoff Street, Northridge, CA 91330-8303, USA

[2]Bermuda Institute of Ocean Sciences, 17 Biological Station, Ferry Reach, St.George's GE 01 Bermuda

[3]Department of Biology, The University of North Carolina at Chapel Hill, Chapel Hill, NC, 27599-3280 USA

[4]University of Rhode Island, Department of Biological Sciences, 120 Flagg Rd. Kingston, RI 02881 USA

* Corresponding Author

nyssa.silbiger@csun.edu

Keywords: Thermal performance curve, gross photosynthesis, dark respiration, calcification, coral, climate change

Summary statement: We apply a thermal performance curve approach to a variety of fitness related parameters in a reef building coral across its geographic range and various functions to improve our understanding of the inherent variability in thermal tolerance.

Abstract

Temperature drives biological responses that scale from the cellular to ecosystem levels and thermal sensitivity will shape organismal functions and population dynamics as the world warms. Reef building corals are sensitive to temperature due to their endosymbiotic relationship with single celled dinoflagellates, with mass mortality events increasing in frequency and magnitude. The purpose of this study was to quantify the thermal sensitivity of important physiological functions of a Caribbean reef-building coral, *Orbicella franksi* through the measurement of thermal performance curves (TPCs). We compared TPC metrics (thermal optimum, critical maximum, activation energy, deactivation energy, and rate at a standardized temperature) between two populations at the northern and southern extent of the geographic range of this species. We further compared essential coral organismal processes (gross photosynthesis, respiration, and calcification) within a site to determine which function is most sensitive to thermal stress using a hierarchical Bayesian modeling approach. We found evidence for differences in thermal performance, which could be due to thermal adaptation or acclimatization, with higher TPC metrics (thermal optimum and critical maximum) in warmer Panama, compared to cooler Bermuda. We also documented the hierarchy in thermal sensitivity of essential organismal functions within a population, with respiration less sensitive than photosynthesis, which was less sensitive than calcification. Understanding thermal performance of corals is essential for projecting coral reef futures, given that key biological functions necessary to sustain coral reef ecosystems are thermally-mediated.

Introduction

Evidence that anthropogenic climate change is impacting the natural world continues to accumulate (Parmesan and Yohe, 2003; Poloczanska et al., 2013). Populations in all types of habitats — aquatic and terrestrial, from the poles to the equator — are responding to warming (Oliver et al., 2018; Walther et al., 2002) and countless other important environmental changes (U S Global Change Research Program, 2019). Essential to improving predictions of organismal to ecosystem responses to environmental change, is the quantification of not only individual/genotype and population response to warming, but also functional sensitivities.

The sensitivity of ecotherms to temperature can be characterized empirically as a Thermal Performance Curve (TPC), which quantifies the shape of the relationship (typically following a Sharpe-Schoolfield model; (Schoolfield et al., 1981; Sharpe and DeMichele, 1977)) between biological rates of "performance" (e.g., respiration or growth) and environmental temperature (Figure 1; Table 1). TPC parameters such as critical minimum (CT_{min}), critical maximum (CT_{max}), and thermal optimum (T_{opt}) describe the limits and optima of a chosen process with changing temperature (Angilletta, 2009; Huey and Kingsolver, 1989; Huey and Stevenson, 1979). The positive and negative slopes on either side of T_{opt} are the rates of activation (E) and deactivation (E_h) energy, respectively, and indicate the sensitivity of the process. Species with high E and E_h (i.e. steeper slopes on either end of the curve) will be most sensitive because they will quickly move from optimal to suboptimal conditions with only small changes in temperature. The rate at a standardized temperature, $b(T_c)$, is often used to compare rates between organisms or functions at a reference temperature (Padfield et al., 2017). Each of these TPC parameters can be compared among populations and species, locations with different thermal histories (e.g., across latitudes), and over time to predict future community composition and the functional consequences of environmental change.

In the context of climate change, applying a TPC approach to quantify thermal adaptation is essentially a space-for-time substitution (Blois et al., 2013; Faber et al., 2018; Pickett, 1989) — a widely used approach when the practical temporal extent of a study cannot match the process of interest. There is extensive evidence of "adaptation" to spatial temperature gradients in a wide range of organisms, from local (e.g., tens of meters) to regional (100s of km) scales (Berkelmans, 2002; Berkelmans and Willis, 1999; Castillo et al., 2012; Oliver and Palumbi, 2011). Such phenotypic gradients presumably reflect an underlying selection gradient and can provide clues about numerous aspects of thermal adaptation, such as fitness costs and other trade-offs and the plausible range of survivable temperatures.

Coral reefs are being severely affected by global warming. Like many other foundation species, the corals that build tropical reefs are being lost in response to anthropogenic warming (Hughes et al., 2017; Hughes et al., 2018b). Coral cover has declined dramatically on reefs worldwide over the last 30 years (from ~60% to <20% on some reefs), in large part due to ocean warming (Bruno and Selig, 2007; De'ath et al., 2012; Gardner et al., 2003; Hughes et al., 2018a) causing mass bleaching, or the loss of the corals' symbiotic dinoflagellates and their nutritional

93 benefits to the host (Oakley and Davy, 2018). While there are numerous local causes of coral loss
94 (e.g., pollution, destructive fishing practices, tourism, etc.), the single most detrimental stressor to
95 date is thermal stress from anomalous heating events (i.e., heatwaves) and its associated
96 complications (i.e., bleaching, disease, reduced calcification etc.; (DeCarlo et al., 2017; Harvell et
97 al., 2002; Hughes et al., 2017)). Reef building corals and their dinoflagellate symbionts live close
98 to their physiological thermal maximum and, as a result, warming of 1°C or more above local
99 mean monthly maxima can reduce fitness and cause tissue loss or whole-colony mortality (Hoegh-
100 Guldberg 1999, Baker et al. 2008), with significant negative implications for reef structure and
101 function (Couch et al., 2017; Hughes et al., 2018b; Stuart-Smith et al., 2018). In the case of corals,
102 there are numerous mechanisms that could enable local thermal adaptation, including genetic
103 adaptation and physiological acclimatization of the host, changes in Symbiodinaceae composition,
104 and the bacterial microbiome (Putnam et al., 2017).

105 Corals have several key physiological traits that scale up to influence ecosystem function.
106 These traits include production, respiration, and calcification, which generate much of the carbon
107 on a coral dominated reef, power coral metabolic processes, and build the 3-dimensional structure
108 of the reef, respectively. Importantly, these traits are likely to have different responses to
109 temperature. For example, coral holobiont photosynthesis is dependent on single celled
110 dinoflagellates (in the family Symbiodiniaceae; (LaJeunesse et al., 2018)). These endosymbionts
111 act as light and temperature sensors for the coral host and typically initiate the cascade of dysbiosis
112 and bleaching through the generation of reactive oxygen species production, due to excess
113 excitation energy in the photosystems under increasing temperatures (Oakley and Davy, 2018).
114 Additionally, different enzymatic machinery is utilized for these different traits, with likely
115 differing thermal optima. Therefore, in comparison, holobiont respiration is likely to be less
116 sensitive to temperature than photosynthesis. Further, because light-enhanced calcification is
117 hypothesized to be dependent on energy supplied by Symbiodiniaceae (Allemand et al., 2011),
118 corals may substantially reduce calcification when production is low (e.g., during bleaching
119 events; (Barkley et al., 2018)). Lastly, the ratios between these different processes can change with
120 temperature and have implications for survival and the long-term persistence of certain coral
121 functions (Coles and Jokiel, 1977).

122 The purpose of this study was to quantify the thermal sensitivity of important physiological
123 functions of a reef-building coral with the goals of 1) comparing responses among colonies

(putative clones) of the Caribbean coral *Orbicella franksi*, between two populations at the northern (cool, Bermuda) and near the southern (warm, Panama) extent of the geographic range of this species and 2) comparing essential coral organismal processes (gross photosynthesis, respiration, and calcification) within a site (Bermuda) to determine which function is most sensitive to thermal stress. We hypothesized that corals in Panama would have higher thermal optima than Bermuda based on thermal history and that respiration rates would be more thermally tolerant than photosynthesis and calcification based on symbiont sensitivity to light and temperature and evidence for their contributions to dysbiosis (Lesser, 2011; Oakley and Davy, 2018; Venn et al., 2008). To test these hypotheses, we quantified TPCs using a set of hierarchical Bayesian models.

Materials and Methods

Study Sites (Panama and Bermuda)

The Bocas del Toro Archipelago is located on the Caribbean coast of Panama at 9°N, 82°W on the border of Costa Rica (Figure 2). It is composed of a complex network of islands and mainland peninsulas fringed by mangroves with well-developed seagrass beds and coral reefs (Collin, 2005). The region hosts a high diversity of scleractinian corals, with 61 species documented, and mean coral coverage of 26.9% (Guzman et al., 2005). Long-term temperature records from shallow fringing reef systems within the Bocas del Toro Archipelago monitored from 1999-2004 document an annual mean seawater temperature of 28.5°C, ranging from a mean of 25.9°C in Jan-Feb to 29.7°C in Sept-Oct (Kaufmann and Thompson, 2005).

Located at approximately 32°N, 64°W, 1049 km (652 nm) southeast of Cape Hatteras (US central east coast), Bermuda's sub-tropical coral reefs represent the northernmost shallow-water reef system in the Atlantic Ocean (Figure 2). Annual reefal temperatures across the shallow reef platform (3–18 m depth) range from 15–30°C (Coates et al., 2013; Locke et al., 2013a), which allows a variety of tropical marine organisms to live in this region, including 38 hermatypic and ahermatypic scleractinian coral species (Locke et al., 2013b). Bermuda is markedly cooler, however, than typical Caribbean reefs. For example, during the wintertime, on average, inshore SST is 8°C cooler in Bermuda than Panama (Figure 2). Maximum temperature in the summer is also >1°C lower in Bermuda than in Panama. Importantly, this has led to minimal impacts of coral bleaching in Bermuda (Cook et al., 1990).

Study Species

Orbicella spp. has been a dominant reef building coral in the Caribbean since at least the late Pleistocene (for ~1.2 million years) (Aronson and Precht, 2001). The *Orbicella* spp. complex has a broad geographic distribution across the western Atlantic, ranging from Brazil in the south to Bermuda in the north (Budd et al., 2012) and is a vital component of Caribbean reefs. The Caribbean has warmed at a rate of 0.27°C per decade between 1985 and 2009 (Chollett et al., 2012), causing mass mortality of *Orbicella* via bleaching and infectious-disease outbreaks (e.g., Bruckner and Hill, 2009; Weil, 2004). *O. franksi* is, therefore, an ideal coral for our study given its abundance in both Panama and Bermuda, its reef-building role, and its recent listing as threatened under the U.S. Endangered Species Act.

Sample Collection

In Bermuda, specimens of *O. franksi* were collected from the reefs at Hog Breaker, which is located on the rim reef of the northern lagoon (32° 27' 26.38"N, 64° 50" 5.1"W; Figure 2), at a depth of 8-12m on Sept. 30, 2017. Bottom seawater temperature at the time of collection was recorded on a Shearwater Petrel dive computer as 26.1°C. In Panama, specimens of *O. franksi* were collected from the reefs at Crawl Cay on Nov. 25, 2017, which sits on the ocean facing side of the archipelago between Isla Bastimentos and Isla Popa (9° 14' 37.8"N 82° 08' 25"W; Figure 2), at a depth of 5-10m. This site was selected based on its distance from the mainland and the town of Bocas del Toro, in order to minimize the impacts of terrestrial runoff and nearshore anthropogenic impacts, and to more closely reflect the conditions of the rim reef collection site in Bermuda. Bottom seawater temperature at the time of collection was recorded on a Shearwater Petrel dive computer as 27.8°C. All samples were collected with a hammer and chisel. Sampled colonies in both locations were separated by a minimum of 5m to reduce the probability of selecting clones.

Samples were brought back to the respective marine laboratory (Bermuda Institute of Ocean Sciences [BIOS] or Smithsonian Tropical Research Institute [STRI]) submerged in seawater in insulated coolers. Once at the lab, the colonies were immediately fragmented with a hammer and chisel into 11 replicate ramets and maintained in seawater flow through systems outside under ambient light and ambient temperature conditions (~27°C and ~28°C in Bermuda and Panama, respectively), where they were allowed to recover for 24-72 hrs. before experimentation. Samples were then moved to a holding tank inside the laboratory in ambient

seawater temperature under greenhouse lights in Bermuda (Sun Blaze T5 High Output Fluorescent Light Fixtures) at 130±6 (mean ± SE, n=9) µmol m^{-2} s^{-1} prior to TPC measurements.

PI Curves

Prior to experimental exposures, replicate coral fragments were used to generate photosynthesis-irradiance curves for each location to determine saturating irradiance for assessing rates of photosynthesis. Fragments were placed in individual acrylic respiration chambers (620mL) with 5µm filtered seawater in Bermuda and 50µm filtered in Panama, with individual temperature (Pt1000) and fiber-optic oxygen probes (Presens dipping probes [DP-PSt7-10-L2.5-ST10-YOP]). Oxygen was measured every second in the coral chambers and blank chambers. Fragments were exposed to nine light levels generated by LED lights hung above the chambers (Arctic-T247 Aquarium LED, OceanRevive): 0, 31, 63, 104, 164, 288, 453, 610, and 747 µmol m^{-2} s^{-1} in Bermuda and 0, 22, 65, 99, 210, 313, 476, 613, and 754 µmol m^{-2} s^{-1} in Panama. Light levels were determined by an underwater cosine corrected sensor (MQ-510 quantum meter Apogee Instruments, spectral range of 389-692 nm ± 5 nm).

Rates of Oxygen flux were extracted using repeated local linear regressions with the package *LoLinR* (Olito et al., 2017) in R (R Core Team, 2013), corrected for chamber volume, blank rates, and normalized to coral surface area calculated by tracing of planar area of the flat *O. franksi* samples using ImageJ (Schneider et al., 2012). *LoLinR* was run with the parameters of L_{pc} for linearity metric (L_{pc} = the sum of the percentile-ranks of the Zmin scores for each component metric) and alpha = 0.2 (minimum window size for fitting the local regressions, which is the proportion of the total observations in the data set) for observations, and thinning of the data from every second to every 20 seconds. A non-linear least squares fit (NLLS;(Marshall and Biscoe, 1980)) for a non-rectangular hyperbola was used to identify PI curve characteristics of each species. This model is as follows:

$$P_{net} = \frac{\phi PAR + \sqrt{(\varphi PPFD + P_{max})2 - 4\Theta\varphi PAR\, P_{max}}}{2\Theta} - R_d , \quad [1]$$

where the parameters are P_{net} and P_{max} (area-based net and maximum gross photosynthetic rates, respectively), R_d (dark respiration, started at min rate in the dark), AQY (φ, apparent quantum

yield), PAR (photosynthetically active radiation), and Theta (Θ, curvature parameter, dimensionless).

These PI curves identified saturating irradiance (I_k) of 110 µmol m^{-2} s^{-1} for Bermuda and 184 µmol m^{-2} s^{-1} for Panama, with no indication of photoinhibition (Figure S1). Subsequent measurements of photosynthetic rates were completed at 553±22 µmol m^{-2} s^{-1} in Bermuda and 623±21 µmol m^{-2} s^{-1} in Panama.

Characterizing Metabolic Thermal Response

For TPC measurements, fragments were placed in individual respiration chambers to measure photosynthesis and dark respiration rate, as light enhanced dark respiration rates (Edmunds and Davies, 1988) (hereafter, respiration or R_d), after ~60 minutes of light exposure. The respirometry setup consisted of ten 620 ml chambers with magnetic stir bars. Samples were measured in a series of runs that consisted of replicate fragments and blank chambers, and included 60 minutes under saturating irradiance, followed by 60 minutes of dark. New fragments from the same colonies (N = 4 colonies/genotypes) were used for each temperature run, resulting in acute TPC curves. Importantly, while these acute and non-ramping TPCs provide good comparative (relative) metrics of thermal responsiveness, they overestimate the metrics relative to samples acclimatized to each temperature, or ramped through all the temperatures (Schulte et al., 2011; Sinclair et al., 2016). We measured net photosynthesis and dark respiration at seven temperatures in Bermuda (24, 26, 27, 29, 31, 32, 34, 36°C) and eleven temperatures in Panama (26, 27, 28, 29, 30, 31, 32, 33, 34, 35, 37°C). Temperature was controlled to ±0.1°C by a thermostat system (Apex Aquacontroller, Neptune Systems) using a chiller (AquaEuroUSA Max Chill-1/13 HP Chiller) and heaters (AccuTherm Heater 300W). Rates of oxygen flux were extracted following the methods described above and gross photosynthesis (GP) was calculated as the absolute values of net photosynthesis plus dark respiration.

In Bermuda only, we also measured light and dark calcification across the seven temperatures. Calcification rates were calculated using the total alkalinity (A_T) anomaly technique (Chisholm and Gattuso, 1991). Water samples (N = 3 replicates) for A_T were collected in thrice rinsed, acid washed 250 mL Nalgene bottles from the temperature-controlled seawater prior to incubation and then again from each chamber (both corals and blanks) after the 60 min incubation. A_T samples were immediately preserved with 100 µL of 50% saturated $HgCl_2$. A_T was analyzed

using open cell potentiometric titrations (Dickson et al., 2007) on a Mettler T5 autotitrator. A certified reference material (CRM, Reference Material for Oceanic CO_2 Measurements, A. Dickson, Scripps Institution of Oceanography) was run at the beginning of each sample set. The accuracy of the titrator was always less than 0.8% off from the standard and the precision was <5 µmol kg^{-1} between sample replicates.

Because calcification from the alkalinity anomaly is the sum of all calcification and dissolution processes in the coral, all exposed skeleton on the corals was covered with parafilm immediately prior to measurements to minimize dissolution of the carbonate framework. Light and dark calcification rates (µmol $CaCO_3$ cm^{-2} h^{-1}) were calculated using the following equation:

$$Calcification = \frac{\Delta A_T \cdot V \cdot \rho}{2 \cdot t \cdot SA}, \quad [2]$$

where ΔA_T (µmol kg^{-1}) is the difference in A_T between the initial and post incubation sample (note: ΔA_T in the blanks was subtracted from the ΔA_T in the coral samples to account for any calcification due to other calcifiers in the seawater), V (cm^3) is the volume of water in the chamber accounting for the volume of the coral, ρ is the density of seawater (average density = 1.023 g cm^{-3}), t (h) is the incubation time (~1 hr), and SA (cm^2) is the surface area of the corals determined tracing of planar area of the flat *O. franksi* samples using ImageJ (Schneider et al., 2012). ΔA_T was divided by 2 because 1 mol of $CaCO_3$ is produced for every 2 mols of A_T. Changes in dissolved inorganic nutrients were assumed to be minor in an hour incubation, making it unnecessary to account for nutrient concentrations in the alkalinity anomaly. Salinity was also measured in the pre- and post-incubation water samples (~37 psu), but no evaporation was noted: the chambers were airtight. We present our results as net calcification (NC = light calcification + dark calcification).

Model Construction

We used Bayesian hierarchical models with Markov Chain Monte Carlo (MCMC) simulations to estimate coral thermal tolerance metrics for GP, R_d, and NC. One outlier in the NC data (temperature = 26 °C) was removed due to contamination of an alkalinity sample. Log(x+1) GP, R_d, and NC rates were fit to modified Sharpe-Schoolfield models for high temperature inactivation (Schoolfield et al., 1981) (Table 1, Fig 1). We ran three separate models to explicitly test the hypotheses that TPC parameters for GP (model 1) and R_d (model 2) differ between the Bermuda and Panama populations, and that TPC parameters differ among the three organismal

functions in Bermuda only (model 3). To get reliable estimates of all TPC parameters, the maximum experimental temperature needs to be high enough to bring the measured rate to near zero. We did not achieve near-zero R_d rates in Panama (highest temperature measured was 37 °C), thus making the Panama versus Bermuda comparison for R_d unreliable. Therefore, for comparisons between populations (Panama versus Bermuda), we only present the GP model in the main text and we included the R_d model results in the supplement (see Figures S2-4). T_{opt} and CT_{max} were both estimated within the MCMC chain. CT_{max} was calculated as the temperature at which there was a 90% loss of maximum rate (i.e. rate at T_{opt}). For detailed model description please see supplemental materials.

Model Fitting and Analysis

We ran our model using MCMC algorithms in JAGS (just another Gibbs sampler) (Plummer, 2003) called from R (R Core Team, 2013) using the R packages, *rjags* (Plummer, 2011) and *dclone* (Sólymos, 2010). We ran three parallel chains of length 2.5M, with a burn-in of 2M, and a thinning parameter of 1/2000 to account for high autocorrelation in the chains, leaving a total of 13,500 samples for inference.

We assessed convergence by checking all trace plots, ensuring that all chains were well-mixed, and calculating Gelman-Rubin statistics (Gelman and Rubin, 1992) for all parameters (all of which were < 1.05). To assess model fit, we used posterior predictive checks by adding a step in each MCMC iteration to simulate data based on our model's posterior predictive distribution and then comparing it to our observed dataset. Goodness of fit was evaluated using Bayesian p-values, which are based on comparing the discrepancies between observed and simulated data. Bayesian p-values for the mean, standard deviation, and coefficient of variance for all models were between 0.49 - 0.53 (close to 0.5), indicating that differences between observed and simulated data are likely due to chance. Lastly, we plotted our observed versus predicted data from the model simulations and they were in close agreement (Fig S5-6).

For our numerically generated posterior samples, we report median values with two-tailed 95% Bayesian credible intervals (BCI) for each parameter (essentially, Bayesian confidence intervals). We used the *compare_levels* function in the *TidyBayes* package (Kay, 2018) to make pairwise comparisons of each parameter among populations and organismal functions. Pairwise comparisons with credible intervals that do not overlap zero are considered to be statistically

different from each other. All R and JAGS code and data will be available on github (https://github.com/njsilbiger/CoralThermalTolerance) and citable at Zenodo upon publication.

Results

Differences in TPC parameters between populations

The Panama and Bermuda coral populations had markedly different functional responses to temperature (Figure 3). Specifically, for GP, the corals from Panama were more thermally tolerant than those from Bermuda, with a 2.17°C higher T_{opt} (0.95 - 3.65°C [95% BCI]) and a 1.59°C higher CT_{max} (0.93 - 2.61 °C [95% BCI]; Figure 4; Figure S7). The Panama population also had higher GP rates overall. At the reference temperature (27°C) the log(x+1) GP rate was 0.24 μmol cm^{-2} hr^{-1} higher (0.13 - 0.32 μmol cm^{-2} hr^{-1} [95% BCI]) in Panama than Bermuda (Figure 4; Figure S7). Panama corals also had a marginally steeper deactivation energy (E_h) than Bermuda corals, meaning GP drops out more quickly in Panama once it reaches its thermal optimum, but the activation energy (E) was the same between the two populations (Figure 4). For dark respiration comparisons between Panama and Bermuda see supplemental material (Figures S2-4).

Differences in TPC parameters among organismal functions within a population

The TPCs among the three organismal functions tested (GP, R_d, and NC) were also substantially different from one another (Figure 5). In Bermuda, the general pattern in thermal tolerance was R_d > GP > NC (Figure 6; Figure S8). Specifically, R_d had the highest T_{opt} (Figure S8) and was 0.67°C (-0.4 - 1.72 °C [95% BCI]) higher than GP and 1.69°C (0.72 - 3.02°C [95% BCI]) higher than NC (Figure 6). While none of the CT_{max} values were statistically different from one another, on average R_d still had the highest CT_{max} (Figure S8). GP had the steepest deactivation energy (E_h) and was 3.15 (1.36 -5.27 [95% BCI]) and 2.92 (0.89 - 5.07 [95% BCI]) higher than NC and R_d, respectively (Figure 6). None of the activation energies (E) were significantly different from one another.

The GP:R_d and NC:GP ratios also varied by temperature (Figure 5b). GP:R_d generally declined with temperature, although it leveled off between approximately 27 and 30°C. The GP:R_d ratio reached 1, where gross photosynthesis and respiration were equal, at 34.9°C. NC:GP followed a unimodal curve, where the highest ratio (i.e, the most efficient calcification per unit production rate) was at 27.9°C.

Variance components in thermal performance metrics

Clone-level variation in TPC metrics was generally low (Figure S9). Variance in $b(T_c)$ due to differences between populations was 3.6× higher than variance due to differences among clones within a site. Similarly, variance in $b(T_c)$ among the three organismal functions was 2.7× higher than variance among clones.

Discussion

Our results indicate that populations with different thermal histories respond differently to acute warming. Specifically, corals in Bermuda were less heat tolerant than those in Panama. Both T_{opt} and CT_{max} were greater for photosynthesis and T_{opt} was also greater for respiration (note the statistical significance of this difference was marginal). These observed differences in thermal tolerance roughly match the difference in the average maximum summertime high at the two locations (Panama maximum temperature is ~1.2°C higher than Bermuda; Figure 2). Importantly, there are several differences in the thermal regimes between Panama and Bermuda, and both the mean and variance in environmental temperature can affect coral metabolism (Putnam and Edmunds, 2011) and thermal sensitivity (e.g., Safaie et al., 2018). While there are several other environmental differences between Bermuda and Panama, a likely explanation for the observed thermal sensitivities is the fairly large (for a tropical and sub-tropical system) differences in temperature (Figure 2). However, the comparison of phenotypic traits between populations in this, or any other latitudinal study, should be interpreted with caution as the results cannot be clearly attributed to temperature alone.

Assuming the local temperature regime is a dominant cause of the observed among-population differences, numerous evolutionary and ecological processes could underlie this environmental matching. First, natural selection for thermally tolerant host genotypes in Panama could lead to adaptation to the local thermal regime and genetic population differentiation (Torda et al., 2017). Second, both the coral host and endosymbiont could be physiologically acclimatized to local temperatures (Brown and Cossins, 2011). Third, numerous epigenetic mechanisms could enable the Panama corals to be more tolerant of extreme high temperatures (Eirin-Lopez and Putnam, 2019). Fourth, the dominant symbionts could be genetically differentiated (Baker et al., 2004), with a more thermally tolerant strain present at the Panama site. Numerous studies have found substitutions of thermally sensitive endosymbionts by more tolerant ones in both space and

time (e.g., Baker et al., 2004; Boulotte et al., 2016). Fifth, it is also possible that differences in the coral-associated microbial community affect responses of host and symbiont to the temperature treatments (Webster and Reusch, 2017). While our study was not designed to tease apart the relative contributions of these or other potential mechanisms leading to less thermally sensitive genotypes at the warmer site, several studies have found evidence supportive of thermal acclimation across spatial gradients (Howells et al., 2012; Sunday et al., 2011).

In addition to differing thermal sensitivity among populations, we also found that there are differences in thermal sensitivity among metabolic processes within populations. Specifically, GP, R_d, and NC all had different thermal optima (T_{opt}), rates of deactivation (E_h), and rates at a reference temperature ($b(T_c)$) (Figure 6). Different enzymatic machinery is utilized for each of these traits (e.g., citrate synthase in respiration, RuBISCo in photosynthesis, and Ca-ATPase in calcification), with some being specific to host or symbiont function. Therefore, in comparison, we hypothesized *a priori* that holobiont respiration was likely to be less sensitive to temperature than photosynthesis, which was supported by our data. Calcification was the least tolerant trait with the lowest thermal optimum. Other coral studies have also demonstrated that calcification is more sensitive to temperature than photosynthesis and respiration (though not using an explicit TPC approach) (e.g., Al-Horani, 2005; Reynaud et al., 2003). For example, at high temperatures, *Galaxea fascicularis* in the Red Sea produced less O_2 than it consumed (i.e. higher respiration than photosynthesis rate) and began to decalcify (Al-Horani, 2005). Together, these results indicate that corals may be able to survive slight increases in warming (e.g., ~1-2°C), but they would still experience declines or even ecological loss of important functions related to fitness, or that are necessary for coral reef ecosystem functioning, such as net ecosystem production and net ecosystem calcification.

The ratios of GP:R_d and NC:GP both varied with temperature (Figure 5). These ratios and how they change with temperature, have implications for survival and the long-term persistence of certain functions. For example, corals need a GP:R_d ratio of greater than 2 to maintain long-term autotrophy (Coles and Jokiel, 1977). Here, we saw GP:R_d generally declined with temperature, a pattern that has been shown in other coral studies (Coles and Jokiel, 1977), and that the GP:R_d dropped below 2 at 32.7°C. Therefore, as ocean temperatures continue to warm, *O. franski* will need to shift to more heterotrophic food sources to survive. The NC:GP ratio had a unimodal response to temperature, with the optimal calcification per unit production rate at 27.9°C.

Calcification and photosynthesis are highly coupled in corals and calcifying macroalgae (Barnes and Chalker, 1990; Gattuso et al., 1999; Goreau, 1959; Schneider and Erez, 2006), although the mechanisms linking them continue to be debated (see, Gattuso et al., 1999; Gattuso et al., 2000). Assessing NC:GP ratios can uncover the amount of CO_2 that can potentially be supplied from calcification to photosynthesis (Gattuso et al., 1999) and how this relationship may change with temperature.

We measured acute TPCs, which can be thought of as an instantaneous thermal "stress test". While short acclimation times such as ours would underestimate absolute acclimation potential of the tested organisms, as they do not have time to fully acclimate, acute TPCs are used widely for comparative analyses (Schulte et al., 2011). For example, a relatively recent database compilation of studies examining thermal performance contains thousands of entries for >200 traits across taxa ranging from microbes to animals, spanning ~16 orders of magnitude in body size extracted from ~300 studies (Dell et al., 2013). These TPC studies have helped uncover constraints on thermal acclimation (Rohr et al., 2018) and develop critical advancements in theory (e.g., Metabolic Theory of Ecology; Brown et al., 2004). Such TPC approaches, when conscious of important assumptions and applying appropriate experimental frameworks (Schulte et al., 2011; Sinclair et al., 2016), can provide useful metrics of comparison between organisms, populations, and species.

While there is a massive body of literature on thermal tolerance of terrestrial and marine organisms (Dell et al., 2011), there is surprisingly less on the thermal performance characteristics of coral reef organisms in an explicit TPC context (but see, Aichelman et al., 2019; Jokiel and Coles, 1977; Jokiel and Coles, 1990; Rodolfo-Metalpa et al., 2014). Understanding thermal performance of corals is essential for projecting coral reef futures, given that key biological functions necessary to sustain coral reef ecosystems (e.g., photosynthesis, respiration, calcification) are thermally-mediated. Here, we advance this area of research by applying the TPC approach to a variety of fitness related parameters in a reef building coral across its geographic range, in a robust statistical framework. We suggest that future studies should incorporate multiple species and representatives from other functional groups in order to better predict ecosystem-level responses to temperature. Understanding how patterns of response differ among genotypes will improve our understanding of the inherent variability in thermal tolerance that exists within and among species and therefore potential cascading effects of biodiversity and genetic diversity loss.

Taken together, these approaches will provide information critical to informing evidence-based management and conservation of these threatened ecosystems in the face of a warming ocean.

Author Contributions

- NJS, JB, GGG, and HP designed the experiment, collected data in Bermuda, provided materials, and edited the manuscript;
- JB and GGG collected data in Panama;
- NJS and HP processed the data;
- NJS statistically analyzed the data.

Acknowledgements

We thank BIOS and STRI for facilities support. A. Chequer, D. Becker, E. Strand, K. Gould, J. Mata-lopez, and several students in the Northeastern University Three Seas Program helped collect and process data. J Yoder provided access to a server for running the Bayesian analyses. This is CSUN marine biology contribution# XXXX.

Competing Interests

The authors have no competing interests

Funding

This research was funded in part by the National Science Foundation (grant OCE #1737071 to JFB), California State University, and the Pembroke Foundation International.

Data Availability

All R and JAGS code and data will be available on github (https://github.com/njsilbiger/CoralThermalTolerance) and citable at Zenodo upon publication.

462 **Table 1:** Equations and parameters used in constructing thermal performance curves and
463 calculating derived quantities.

Model/Derived Quantities	**Equation**
Modified Sharpe-Schoolfield for high temperature inactivation	$log(rate) = b(T_c) + E(\frac{1}{T_c} - \frac{1}{k \cdot T_i}) - log(1 + e^{Eh\,(\frac{1}{K \cdot Th} - \frac{1}{K \cdot T_i})})$
Thermal optimum	$Topt = (\frac{Eh \cdot Th}{Eh + (K \cdot Th_k \cdot log(\frac{Eh}{E} - 1))})$
Parameters	**Description**
$b(T_c)$	Log rate at a constant temperature (µmol cm^{-2} hr^{-1})
E	Activation energy (electron volts, eV)
Eh	Temperature-induced inactivation of enzyme kinetics past *Th* for each population (electron volts, eV)
K	Boltzmann constant (8.62×10^{-5} eV K^{-1})
T_c	T_c is the reference temperature at which no low or high temperature inactivation is experienced (defined here as 300.15 K or 27°C)
T_h	Temperature (K) at which half the enzymes are inactivated
T_i	Temperature *i* in Kelvin (K)

464
465
466
467
468
469
470
471
472
473
474
475

476 **Figures**

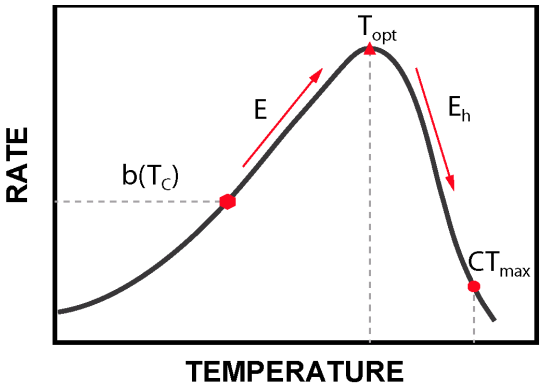

477

478 **Figure 1.** Thermal performance curve characteristics, with comparative temperature metrics
479 identified by the red symbols.

480

481

482

483

484

485

486

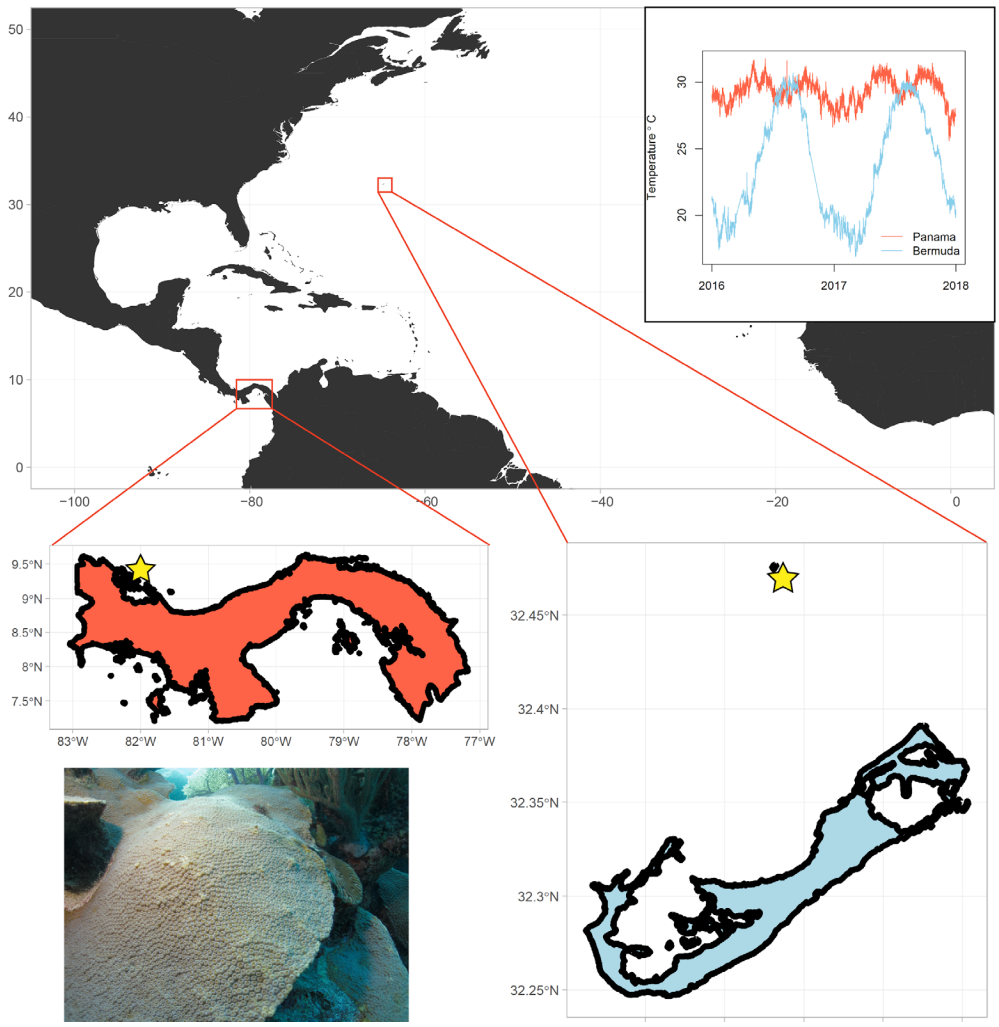

Figure 2. Map of study sites, thermal histories, and image of *Orbicella franski*. Yellow stars in the Panama (orange) and Bermuda (blue) maps indicate collection sites. Inset in the top right shows the thermal histories for each location (Data sets provided by the Physical Monitoring Program of the Smithsonian Tropical Research Institute; NOAA National Data Buoy Center) and inset on the bottom left is an image of *O. franksi* from the collection site in Bermuda (PC: N. Silbiger).

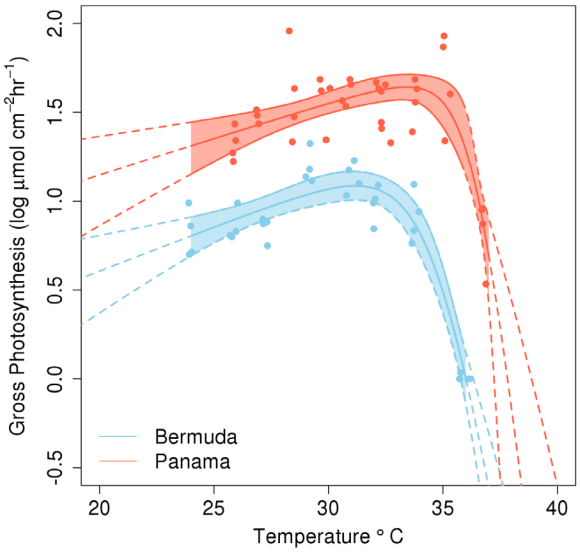

Figure 3. Thermal performance curves of log(x+1) gross photosynthesis rates (µmol O_2 cm^{-2} hr^{-1}) from Panama (orange) and Bermuda (blue). Each dot represents an individual fragment (n = 28 in Bermuda; n = 44 in Panama) of *Orbicella franski* from 4 putative clones. Lines are medians ± 95% BCI drawn from the posterior distribution. The shaded regions are the temperatures where data were collected.

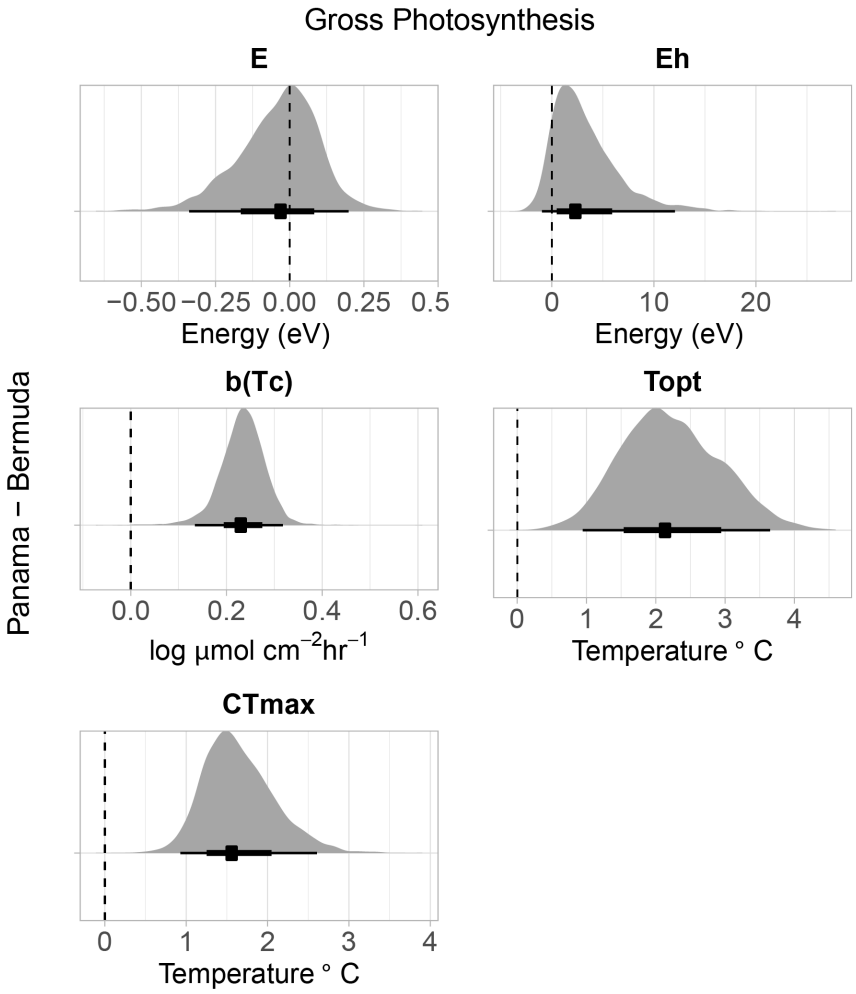

Figure 4. Pairwise comparisons of thermal performance metrics from Panama and Bermuda for gross photosynthesis. Dot and whiskers below each distribution are the median and 95% BCI for each parameter. If the whiskers do not cross the dashed vertical line at 0 then the populations are considered to be statistically different from one another. Positive differences indicate the metric is higher in Panama than Bermuda corals.

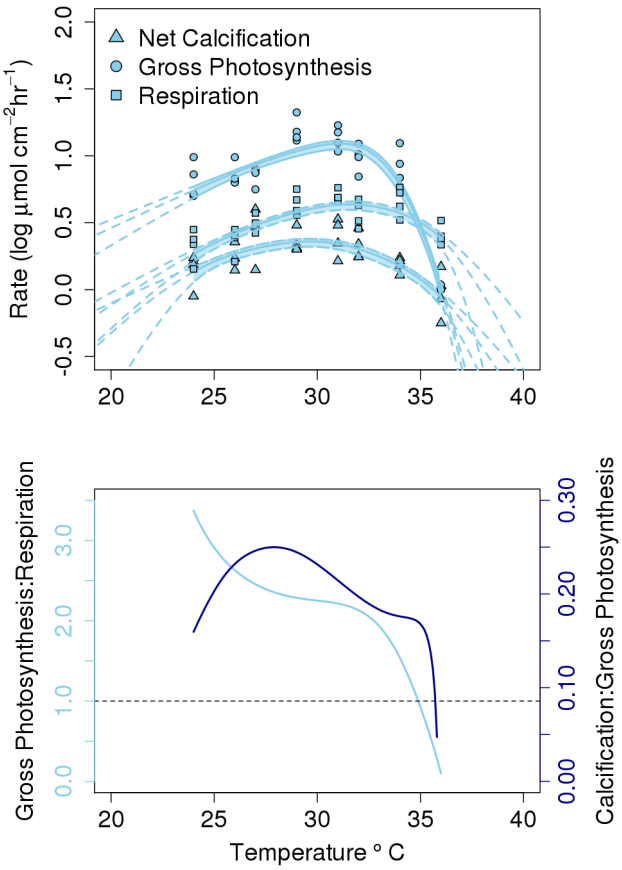

542
543
544

545 **Figure 5. (A)** Thermal performance curves of log(x+1) gross photosynthesis (circles), dark
546 respiration (squares), and net calcification (triangles) rates (µmol O_2 or $CaCO_3$ cm^{-2} hr^{-1}). Each dot
547 represents an individual fragment (n = 28) of *Orbicella franski* from 4 putative clones across 7
548 temperatures. Lines are medians ± 95% BCI drawn from the posterior distribution. The shaded
549 regions are the temperatures where data were collected. **(B)** GP:R (light blue) and NC:GP (dark
550 blue) lines by temperature. Lines are from the best fit (median) from the model (a) and the rates
551 were back transformed before taking the ratio. Dashed horizontal line is at a GP:R = 1. Any value
552 <1 indicates that the dark respiration rate is higher than the gross photosynthesis rate.
553
554
555
556

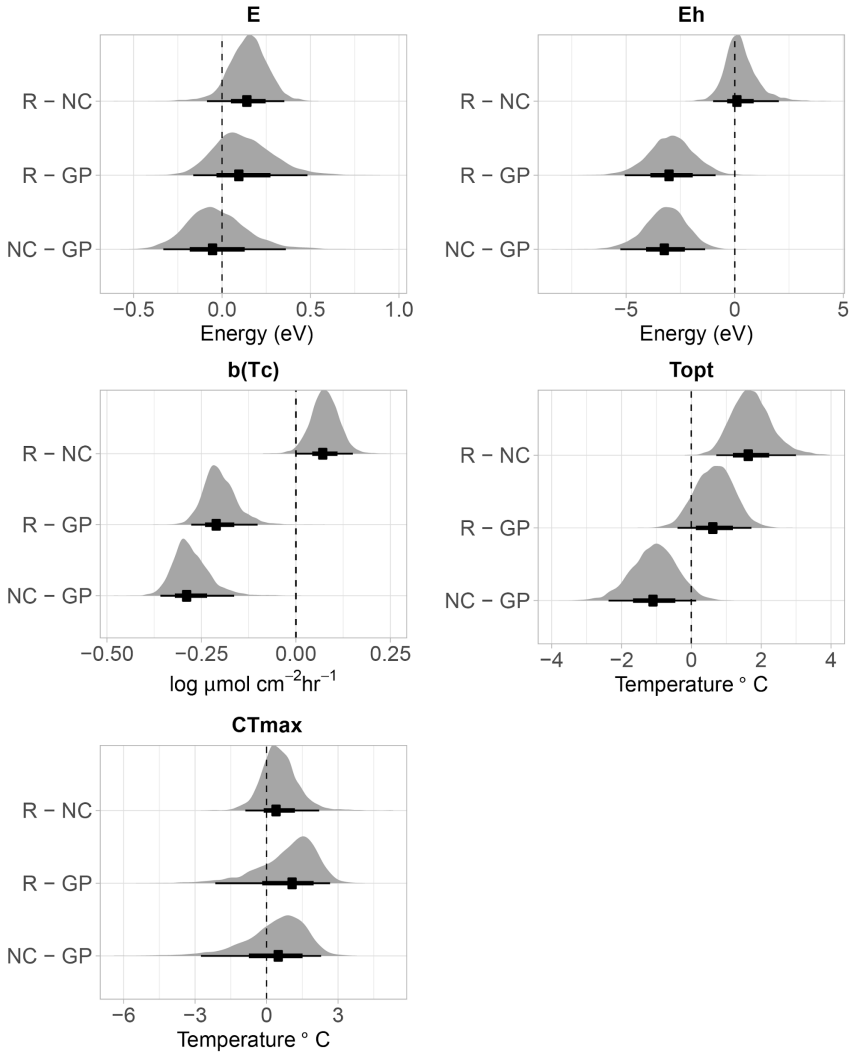

Figure 6. Pairwise comparisons of thermal performance metrics from Bermuda comparing the three organismal functions measured. R is light enhanced dark respiration, GP is gross photosynthesis, and NC is net calcification. Dot and whiskers below each distribution are the median and 95% BCI for each parameter. If the whiskers do not cross the dashed vertical line at 0 then the functions are considered to be statistically different from one another.

References

Aichelman, H. E., Zimmerman, R. C. and Barshis, D. J. (2019). Adaptive signatures in thermal performance of the temperate coral *Astrangia poculata* (Ellis & Solander, 1786). *J. Exp. Biol.* jeb.189225.

Al-Horani, F. A. (2005). Effects of changing seawater temperature on photosynthesis and calcification in the scleractinian coral *Galaxea fascicularis*, measured with O_2, Ca^{2+} and pH microsensors. *Sci. Mar.* **69**, 347–354.

Allemand, D., Tambutté, É., Zoccola, D. and Tambutté, S. (2011). Coral Calcification, Cells to Reefs. In *Coral Reefs: An Ecosystem in Transition* (ed. Dubinsky, Z.) and Stambler, N.), pp. 119–150. Dordrecht: Springer Netherlands.

Angilletta, M. J. (2009). Thermoregulation. In *Thermal Adaptation*, Oxford: Oxford University Press.

Aronson, R. B. and Precht, W. F. (2001). Evolutionary paleoecology: the ecological context of macroevolutionary change. In *Evolutionary paleoecology of Caribbean coral reefs* (ed. Allmon, W. D.) and Bottjer, D. J.), pp. 171–233. New York : Columbia University Press,.

Baker, A. C., Starger, C. J., McClanahan, T. R. and Glynn, P. W. (2004). Coral reefs: corals' adaptive response to climate change. *Nature* **430**, 741.

Barkley, H. C., Cohen, A. L., Mollica, N. R., Brainard, R. E., Rivera, H. E., DeCarlo, T. M., Lohmann, G. P., Drenkard, E. J., Alpert, A. E., Young, C. W., et al. (2018). Repeat bleaching of a central Pacific coral reef over the past six decades (1960-2016). *Commun Biol* **1**, 177.

Barnes, D. and Chalker, B. E. (1990). *Calcification and photosynthesis in reef-building corals and algae*. (ed. Dubinsky, Z.) Coral reefs. Elsevier.

Berkelmans, R. (2002). Time-integrated thermal bleaching thresholds of reefs and their variation on the Great Barrier Reef. *Mar. Ecol. Prog. Ser.* **229**, 73–82.

Berkelmans, R. and Willis, B. L. (1999). Seasonal and local spatial patterns in the upper thermal limits of corals on the inshore Central Great Barrier Reef. *Coral Reefs* **18**, 219–228.

Blois, J. L., Williams, J. W., Fitzpatrick, M. C., Jackson, S. T. and Ferrier, S. (2013). Space can substitute for time in predicting climate-change effects on biodiversity. *Proc. Natl. Acad. Sci. U. S. A.* **110**, 9374–9379.

Boulotte, N. M., Dalton, S. J., Carroll, A. G., Harrison, P. L., Putnam, H. M., Peplow, L. M. and van Oppen, M. J. H. (2016). Exploring the Symbiodinium rare biosphere provides evidence for symbiont switching in reef-building corals. *The ISME Journal* **10**, 2693–2701.

Brown, B. E. and Cossins, A. R. (2011). The Potential for Temperature Acclimatisation of Reef Corals in the Face of Climate Change. In *Coral Reefs: An Ecosystem in Transition* (ed.

Dubinsky, Z.) and Stambler, N.), pp. 421–433. Dordrecht: Springer Netherlands.

Brown, J. H., Gillooly, J. F., Allen, A. P., Savage, V. M. and West, G. B. (2004). Toward a metabolic theory of ecology. *Ecology* **85**, 1771–1789.

Bruckner, A. W. and Hill, R. L. (2009). Ten years of change to coral communities off Mona and Desecheo Islands, Puerto Rico, from disease and bleaching. *Diseases of Aquatic Organisms* **87**, 19–31.

Bruno, J. F. and Selig, E. R. (2007). Regional decline of coral cover in the Indo-Pacific: timing, extent, and subregional comparisons. *PLoS One* **2**, e711.

Budd, A. F., Fukami, H., Smith, N. D. and Knowlton, N. (2012). Taxonomic classification of the reef coral family Mussidae (Cnidaria: Anthozoa: Scleractinia). *Zool. J. Linn. Soc.* **166**, 465–529.

Castillo, K. D., Ries, J. B., Weiss, J. M. and Lima, F. P. (2012). Decline of forereef corals in response to recent warming linked to history of thermal exposure. *Nat. Clim. Chang.* **2**, 756–760.

Chisholm, J. R. M. and Gattuso, J.-P. (1991). Validation of the alkalinity anomaly technique for investigating calcification of photosynthesis in coral reef communities. *Limnol. Oceanogr.* **36**, 1232–1239.

Chollett, I., Mumby, P. J., Müller-Karger, F. E. and Hu, C. (2012). Physical environments of the Caribbean Sea. *Limnol. Oceanogr.* **57**, 1233–1244.

Coates, K. A., Fourqurean, J. W., Judson Kenworthy, W., Logan, A., Manuel, S. A. and Smith, S. R. (2013). Introduction to Bermuda: Geology, Oceanography and Climate. In *Coral Reefs of the World*, pp. 115–133.

Coles, S. L. and Jokiel, P. L. (1977). Effects of temperature on photosynthesis and respiration in hermatypic corals. *Mar. Biol.* **43**, 209–216.

Collin, R. (2005). Ecological monitoring and biodiversity surveys at the Smithsonian Tropical Research Institute's Bocas del Toro research station. *Caribb. J. Sci.* **41**, 367–373.

Cook, C. B., Logan, A., Ward, J., Luckhurst, B. and Berg, C. J. (1990). Elevated temperatures and bleaching on a high latitude coral reef: the 1988 Bermuda event. *Coral Reefs* **9**, 45–49.

Couch, C. S., Burns, J. H. R., Liu, G., Steward, K., Gutlay, T. N., Kenyon, J., Eakin, C. M. and Kosaki, R. K. (2017). Mass coral bleaching due to unprecedented marine heatwave in Papahānaumokuākea Marine National Monument (Northwestern Hawaiian Islands). *PLoS One* **12**, e0185121.

De'ath, G., Fabricius, K. E., Sweatman, H. and Puotinen, M. (2012). The 27--year decline of coral cover on the Great Barrier Reef and its causes. *Proceedings of the National Academy*

639 *of Sciences* 201208909.

640 **DeCarlo, T. M., Cohen, A. L., Wong, G. T. F., Shiah, F.-K., Lentz, S. J., Davis, K. A.,**
641 **Shamberger, K. E. F. and Lohmann, P.** (2017). Community production modulates coral
642 reef pH and the sensitivity of ecosystem calcification to ocean acidification: Production
643 modulates pH and calcification. *J. Geophys. Res. C: Oceans* **122**, 745–761.

644 **Dell, A. I., Pawar, S. and Savage, V. M.** (2011). Systematic variation in the temperature
645 dependence of physiological and ecological traits. *Proc. Natl. Acad. Sci. U. S. A.* **108**,
646 10591–10596.

647 **Dell, A. I., Pawar, S. and Savage, V. M.** (2013). The thermal dependence of biological traits:
648 Ecological Archives E094-108. *Ecology* **94**, 1205–1206.

649 **Dickson, A. G., Sabine, C. L. and Christian, J. R.** (2007). Guide to best practices for ocean
650 CO2 measurements.

651 **Edmunds, P. J. and Davies, P. S.** (1988). Post-illumination stimulation of respiration rate in the
652 coral Porites porites. *Coral Reefs* **7**, 7–9.

653 **Eirin-Lopez, J. M. and Putnam, H. M.** (2019). Marine Environmental Epigenetics. *Ann. Rev.*
654 *Mar. Sci.* **11**, 335–368.

655 **Faber, J., Quadros, A. F. and Zimmer, M.** (2018). A Space-For-Time approach to study the
656 effects of increasing temperature on leaf litter decomposition under natural conditions. *Soil*
657 *Biol. Biochem.* **123**, 250–256.

658 **Gardner, T. A., Côté, I. M., Gill, J. A., Grant, A. and Watkinson, A. R.** (2003). Long-term
659 region-wide declines in Caribbean corals. *Science* **301**, 958–960.

660 **Gattuso, J. P., Allemand, D. and Frankignoulle, M.** (1999). Photosynthesis and Calcification
661 at Cellular, Organismal and Community Levels in Coral Reefs: A Review on Interactions
662 and Control by Carbonate Chemistry. *Integr. Comp. Biol.* **39**, 160–183.

663 **Gattuso, J. P., Reynaud-Vaganay, S., Furla, P., Romaine-Lioud, S., Jaubert, J., Bourge, I.**
664 **and Frankignoulle, M.** (2000). Calcification does not stimulate photosynthesis in the
665 zooxanthellate scleractinian coral Stylophora pistillata. *Limnol. Oceanogr.* **45**, 246–250.

666 **Gelman, A. and Rubin, D. B.** (1992). Inference from Iterative Simulation Using Multiple
667 Sequences. *Stat. Sci.* **7**, 457–472.

668 **Goreau, T. F.** (1959). The physiology of skeleton formation in corals.I. A methods for
669 measuring the rate of calcium deposition by corals under different conditions. *Biol. Bull.*
670 **116**, 59–75.

671 **Guzman, H. M., Barnes, P. A. G., Lovelock, C. E. and Feller, I. C.** (2005). A site description
672 of the CARICOMP mangrove, seagrass and coral reef sites in Bocas del Toro, Panama.
673 *Journal of Caribbean Science* **41**, 430–440.

674 **Harvell, C. D., Mitchell, C. E., Ward, J. R., Altizer, S., Dobson, A. P., Ostfeld, R. S. and**
675 **Samuel, M. D.** (2002). Climate warming and disease risks for terrestrial and marine biota.
676 *Science* **296**, 2158–2162.

677 **Howells, E. J., Beltran, V. H., Larsen, N. W., Bay, L. K., Willis, B. L. and van Oppen, M. J.**
678 **H.** (2012). Coral thermal tolerance shaped by local adaptation of photosymbionts. *Nature*
679 *Climate Change* **2**, 116–120.

680 **Huey, R. B. and Kingsolver, J. G.** (1989). Evolution of thermal sensitivity of ectotherm
681 performance. *Trends Ecol. Evol.* **4**, 131–135.

682 **Huey, R. B. and Stevenson, R. D.** (1979). Integrating Thermal Physiology and Ecology of
683 Ectotherms: A Discussion of Approaches. *Integr. Comp. Biol.* **19**, 357–366.

684 **Hughes, T. P., Kerry, J. T., Álvarez-Noriega, M., Álvarez-Romero, J. G., Anderson, K. D.,**
685 **Baird, A. H., Babcock, R. C., Beger, M., Bellwood, D. R., Berkelmans, R., et al.** (2017).
686 Global warming and recurrent mass bleaching of corals. *Nature* **543**, 373–377.

687 **Hughes, T. P., Anderson, K. D., Connolly, S. R., Heron, S. F., Kerry, J. T., Lough, J. M.,**
688 **Baird, A. H., Baum, J. K., Berumen, M. L., Bridge, T. C., et al.** (2018a). Spatial and
689 temporal patterns of mass bleaching of corals in the Anthropocene. *Science* **359**, 80–83.

690 **Hughes, T. P., Kerry, J. T., Baird, A. H., Connolly, S. R., Dietzel, A., Eakin, C. M., Heron,**
691 **S. F., Hoey, A. S., Hoogenboom, M. O., Liu, G., et al.** (2018b). Global warming
692 transforms coral reef assemblages. *Nature* **556**, 492–496.

693 **Jokiel, P. L. and Coles, S. L.** (1977). Effects of temperature on the mortality and growth of
694 Hawaiian reef corals. *Mar. Biol.* **43**, 201–208.

695 **Jokiel, P. L. and Coles, S. L.** (1990). Response of Hawaiian and other Indo-Pacific reef corals
696 to elevated temperature. *Coral Reefs* **8**, 155–162.

697 **Kaufmann, K. W. and Thompson, R. C.** (2005). Water temperature variation and the
698 meteorological and hydrographic environment of Bocas del Toro, Panama. *Journal of*
699 *Caribbean Science* **41**, 392–413.

700 **Kay, M.** (2018). *tidybayes: Tidy Data and Geoms for Bayesian Models*.

701 **LaJeunesse, T. C., Parkinson, J. E., Gabrielson, P. W., Jeong, H. J., Reimer, J. D., Voolstra,**
702 **C. R. and Santos, S. R.** (2018). Systematic Revision of Symbiodiniaceae Highlights the
703 Antiquity and Diversity of Coral Endosymbionts. *Curr. Biol.* **28**, 2570–2580.e6.

704 **Lesser, M. P.** (2011). Coral Bleaching: Causes and Mechanisms. In *Coral Reefs: An Ecosystem*
705 *in Transition* (ed. Dubinsky, Z.) and Stambler, N.), pp. 405–419. Dordrecht: Springer
706 Netherlands.

707 **Locke, J. M., Coates, K. A., Bilewitch, J. P., Holland, L. P., Pitt, J. M., Smith, S. R. and**
708 **Trapido-Rosenthal, H. G.** (2013a). Biogeography, Biodiversity and Connectivity of

709 Bermuda's Coral Reefs. In *Coral Reefs of the World*, pp. 153–172.

710 **Locke, J. M., Bilewitch, J. P. and Coates, K. A.** (2013b). Scleractinia, Octocorallia and
711 Antipatharia of Bermuda's Reefs and Deep-Water Coral Communities: A Taxonomic
712 Perspective Including New Records. In *Coral Reefs of the World*, pp. 189–200.

713 **Marshall, B. and Biscoe, P. V.** (1980). A Model for C3 Leaves Describing the Dependence of
714 Net Photosynthesis on Irradiance. *J. Exp. Bot.* **31**, 29–39.

715 **Oakley, C. A. and Davy, S. K.** (2018). Cell Biology of Coral Bleaching. In *Coral Bleaching:*
716 *Patterns, Processes, Causes and Consequences* (ed. van Oppen, M. J. H.) and Lough, J.
717 M.), pp. 189–211. Cham: Springer International Publishing.

718 **Olito, C., White, C. R., Marshall, D. J. and Barneche, D. R.** (2017). Estimating monotonic
719 rates from biological data using local linear regression. *J. Exp. Biol.* **220**, 759–764.

720 **Oliver, T. A. and Palumbi, S. R.** (2011). Do fluctuating temperature environments elevate coral
721 thermal tolerance? *Coral Reefs* **30**, 429–440.

722 **Oliver, E. C. J., Donat, M. G., Burrows, M. T., Moore, P. J., Smale, D. A., Alexander, L. V.,**
723 **Benthuysen, J. A., Feng, M., Sen Gupta, A., Hobday, A. J., et al.** (2018). Longer and
724 more frequent marine heatwaves over the past century. *Nat. Commun.* **9**, 1324.

725 **Padfield, D., Lowe, C., Buckling, A., Ffrench-Constant, R., Student Research Team,**
726 **Jennings, S., Shelley, F., Ólafsson, J. S. and Yvon-Durocher, G.** (2017). Metabolic
727 compensation constrains the temperature dependence of gross primary production. *Ecol.*
728 *Lett.* **20**, 1250–1260.

729 **Parmesan, C. and Yohe, G.** (2003). A globally coherent fingerprint of climate change impacts
730 across natural systems. *Nature* **421**, 37–42.

731 **Pickett, S. T. A.** (1989). Space-for-Time Substitution as an Alternative to Long-Term Studies. In
732 *Long-Term Studies in Ecology: Approaches and Alternatives* (ed. Likens, G. E.), pp. 110–
733 135. New York, NY: Springer New York.

734 **Plummer, M.** (2003). JAGS: A program for analysis of Bayesian graphical models using Gibbs
735 sampling. In *Proceedings of the 3rd international workshop on distributed statistical*
736 *computing*, Vienna, Austria.

737 **Plummer, M.** (2011). rjags: Bayesian graphical models using MCMC. R package version 2.2. 0-
738 4.

739 **Poloczanska, E. S., Brown, C. J., Sydeman, W. J., Kiessling, W., Schoeman, D. S., Moore,**
740 **P. J., Brander, K., Bruno, J. F., Buckley, L. B., Burrows, M. T., et al.** (2013). Global
741 imprint of climate change on marine life. *Nat. Clim. Chang.* **3**, 919.

742 **Putnam, H. M. and Edmunds, P. J.** (2011). The physiological response of reef corals to diel
743 fluctuations in seawater temperature. *J. Exp. Mar. Bio. Ecol.* **396**, 216–223.

744 **Putnam, H. M., Barott, K. L., Ainsworth, T. D. and Gates, R. D.** (2017). The Vulnerability
745 and Resilience of Reef-Building Corals. *Curr. Biol.* **27**, R528–R540.

746 **R Core Team** (2013). R: A language and environment for statistical computing.

747 **Reynaud, S., Leclercq, N., Romaine-Lioud, S., Ferrier-Pages, C., Jaubert, J. and Gattuso,**
748 **J.-P.** (2003). Interacting effects of CO2 partial pressure and temperature on photosynthesis
749 and calcification in a scleractinian coral. *Glob. Chang. Biol.* **9**, 1660–1668.

750 **Rodolfo-Metalpa, R., Hoogenboom, M. O., Rottier, C., Ramos-Esplá, A., Baker, A. C., Fine,**
751 **M. and Ferrier-Pagès, C.** (2014). Thermally tolerant corals have limited capacity to
752 acclimatize to future warming. *Glob. Chang. Biol.* **20**, 3036–3049.

753 **Rohr, J. R., Civitello, D. J., Cohen, J. M., Roznik, E. A., Sinervo, B. and Dell, A. I.** (2018).
754 The complex drivers of thermal acclimation and breadth in ectotherms. *Ecol. Lett.* **21**,
755 1425–1439.

756 **Safaie, A., Silbiger, N. J., McClanahan, T. R., Pawlak, G., Barshis, D. J., Hench, J. L.,**
757 **Rogers, J. S., Williams, G. J. and Davis, K. A.** (2018). High frequency temperature
758 variability reduces the risk of coral bleaching. *Nat. Commun.* **9**, 1671.

759 **Schneider, K. and Erez, J.** (2006). The effect of carbonate chemistry on calcification and
760 photosynthesis in the hermatypic coral Acropora eurystoma. *Limnol. Oceanogr.* **51**, 1284–
761 1293.

762 **Schneider, C. A., Rasband, W. S. and Eliceiri, K. W.** (2012). NIH Image to ImageJ: 25 years
763 of image analysis. *Nat. Methods* **9**, 671–675.

764 **Schoolfield, R. M., Sharpe, P. J. and Magnuson, C. E.** (1981). Non-linear regression of
765 biological temperature-dependent rate models based on absolute reaction-rate theory. *J.*
766 *Theor. Biol.* **88**, 719–731.

767 **Schulte, P. M., Healy, T. M. and Fangue, N. A.** (2011). Thermal performance curves,
768 phenotypic plasticity, and the time scales of temperature exposure. *Integr. Comp. Biol.* **51**,
769 691–702.

770 **Sharpe, P. J. H. and DeMichele, D. W.** (1977). Reaction kinetics of poikilotherm development.
771 *J. Theor. Biol.* **64**, 649–670.

772 **Sinclair, B. J., Marshall, K. E., Sewell, M. A., Levesque, D. L., Willett, C. S., Slotsbo, S.,**
773 **Dong, Y., Harley, C. D. G., Marshall, D. J., Helmuth, B. S., et al.** (2016). Can we predict
774 ectotherm responses to climate change using thermal performance curves and body
775 temperatures? *Ecol. Lett.* **19**, 1372–1385.

776 **Sólymos, P.** (2010). dclone: Data Cloning in R. *R J.* **2**,.

777 **Stuart-Smith, R. D., Brown, C. J., Ceccarelli, D. M. and Edgar, G. J.** (2018). Ecosystem
778 restructuring along the Great Barrier Reef following mass coral bleaching. *Nature* **560**, 92.

779 **Sunday, J. M., Bates, A. E. and Dulvy, N. K.** (2011). Global analysis of thermal tolerance and
780 latitude in ectotherms. *Proc. Biol. Sci.* **278**, 1823–1830.

781 **Torda, G., Donelson, J. M., Aranda, M., Barshis, D. J., Bay, L., Berumen, M. L., Bourne,**
782 **D. G., Cantin, N., Foret, S., Matz, M., et al.** (2017). Rapid adaptive responses to climate
783 change in corals. *Nature Climate Change* **7**, 627–636.

784 **U S Global Change Research Program** (2019). *The Climate Report: National Climate*
785 *Assessment-impacts, Risks, and Adaptation in the United States*. Melville House.

786 **Venn, A. A., Loram, J. E. and Douglas, A. E.** (2008). Photosynthetic symbioses in animals. *J.*
787 *Exp. Bot.* **59**, 1069–1080.

788 **Walther, G.-R., Post, E., Convey, P., Menzel, A., Parmesan, C., Beebee, T. J. C., Fromentin,**
789 **J.-M., Hoegh-Guldberg, O. and Bairlein, F.** (2002). Ecological responses to recent
790 climate change. *Nature* **416**, 389–395.

791 **Webster, N. S. and Reusch, T. B. H.** (2017). Microbial contributions to the persistence of coral
792 reefs. *The ISME Journal* **11**, 2167–2174.

793 **Weil, E.** (2004). Coral Reef Diseases in the Wider Caribbean. *Coral Health and Disease* 35–68.

794